Experimental study of the structure of the plasma-current sheath on the PF-1000 facility

2012 Plasma Phys. Control. Fusion 54 025010

(http://iopscience.iop.org/0741-3335/54/2/025010)

Plasma Phys. Control. Fusion **54** (2012) 025010 (14pp) doi:10.1088/0741-3335/54/2/025010

Experimental study of the structure of the plasma-current sheath on the PF-1000 facility

V Krauz[1], K Mitrofanov[2], M Scholz[3], M Paduch[3], L Karpinski[3], E Zielinska[3] and P Kubes[4]

[1] NRC 'Kurchatov Institute', Moscow, Russia
[2] SRC RF TRINITI, Troitsk, Moscow Oblast, Russia
[3] IPPLM, Warsaw, Poland
[4] CVUT, Prague, Czech Republic

E-mail: krauz@nfi.kiae.ru

Received 28 September 2011, in final form 3 December 2011
Published 19 January 2012
Online at stacks.iop.org/PPCF/54/025010

Abstract
The results of studies of the plasma-current sheath structure on the PF-1000 facility in the stage close to the instant of pinch formation are presented. The measurements were performed using various modifications of the calibrated magnetic probes. Studies of the influence of the probe shape and dimensions on the measurements accuracy were done. The current flowing in the converging sheath at a distance of 40 mm from the axis of the facility electrodes was measured. In the optimal operating modes, this current is equal to the total discharge current, which indicates the high efficiency of current transportation toward the axis. In such shots a compact high-quality sheath forms with shock wave in front of the magnetic piston. It is shown that the neutron yield depends on the current compressed onto the axis. This dependence agrees well with the known scaling, $Y_n \sim I^4$. The use of the total discharge current in constructing the current scaling, especially for facilities with a large stored energy, is unjustified.

(Some figures may appear in colour only in the online journal)

1. Introduction

It is well known that, in plasma focus (PF) systems, the intensity of ionizing radiation emitted from the pinch region depends strongly on the pinch current I. In particular, the experimental neutron scaling based on measurements performed at facilities with a stored energy, W, from several units of kilojoules to a few hundred kilojoules has the form $Y_n \sim I^{3.2-5}$ [1–3]. For this energy range the scaling agrees well with another well-known experimental scaling $Y_n \sim W^2$. Such dependence, slightly divergent in power from 2.1 to 2.5, was found on many devices in the early stages of PF-studies [4–6]. In the beginning of the 1970s H Rapp analyzed the results obtained on more than 10 facilities in the world, and showed that this scaling has a general character [7]. Later this scaling has been expanded to sub-kJ machines [8, 9]. However, experiments carried out on megajoule facilities [10–12] demonstrated that, when the energy stored in the capacitor bank exceeded a certain critical value, the scaling in terms of energy was violated and the neutron yield was saturated at a level of $\sim 10^{11}$–10^{12} neutrons/shot. The nature of this effect is one of the key subjects of study in PF systems; in particular, it is of great importance to find out whether saturation is related to natural physical constraints or determined by disadvantages of the facility design [13].

We believe that saturation is not related to any physical constraints. At least, on the Z-facility (Sandia National Laboratories), a neutron yield of $\sim 5 \times 10^{13}$ D–D neutrons per shot was achieved, however, at a very high discharge current of 17 MA [14]. Although the above scaling was not satisfied in this case, these experiments demonstrated the fundamental possibility of obtaining high neutron yields at realistic currents in Z-pinch systems.

The problem of achieving high discharge currents in PF systems is being actively discussed. In particular, in [15] it was asserted that the further increase in the current amplitude can

be provided only by increasing the initial discharge voltage, which inevitably leads to a gradual conversion of PF systems to fast Z-pinch configurations and the loss of one of the main advantages of PF systems, namely, the simplicity of design. In contrast, calculations, made in the framework of the Lee model [16–18], show that there was no saturation in pinch current and Y_n: they continue to rise with condenser bank capacity C_0 although at a slower rate. But these calculations, made for PF-1000 parameters, show also, that, in spite of high power in neutron scaling ($Y_n \sim I_{pinch}^{4.7}$ and $Y_n \sim I_{peak}^{3.9}$) [17], the D–D neutron yield $Y_n \sim 10^{13}$ can be achieved only at W close to 19 MJ [16].

In this study, we do not consider this problem in detail, because it obviously requires more thorough examination. There is another (no less important) problem that manifests itself already at currents achievable in the existing facilities—the problem of the transportation efficiency of the total discharge current toward the system axis, where the pinch forms. The saturation effect can manifest itself if a fraction of the total PF current flows beyond the pinch. Measurements of the current distribution performed on the megajoule PF facility at Frascati showed that a fraction of the total current flowed in the residual plasma near the PF insulator and did not contribute to the process of pinch compression [19]. Thus, despite infringement of the neutron scaling in terms of energy, scaling in terms of the current flowing in the sheath continued to be valid. It became clear that the current in the sheath (or the pinch current) so far does not always coincide with a total discharge current. In [20] the distinction of these currents for various installations is estimated. It was concluded that (i) the relevant parameter of neutron production is the sheath current I_{sh} and not total current I_t and (ii) all effectively operated facilities at a comparative low level of input energy have the relation I_{sh}/I_t close to 1.

At the same time the results reported in [19] and obtained on very fast high-voltage facility SPEED2 [21] have shown that this problem becomes more challenging with increasing discharge energy. The same situation was observed on the PF-3 facility (Kurchatov Institute, Moscow), where absolutely calibrated magnetic probes were used to measure the current distribution in PF experiments with noble gases. The results of probe measurements showed that, in the PF-3 experiments carried out with neon, only a fraction of the total discharge current contributed to the process of pinch compression [22–24].

The efficiency of current transportation toward the system axis depends substantially on the efficiency of the 'snowplow' mechanism. Poor snowplowing of the neutral gas by the magnetic piston in the outward expansion and the 'runaway' stages can result in the high density of the residual plasma behind the plasma-current sheath (PCS) and, accordingly, in substantial current leakages. The spatial distribution of the plasma density and current in the final stage of plasma compression should substantially affect plasma stability and the processes responsible for magnetic energy dissipation and radiation generation. Therefore, studies of the PCS structure are of great importance. The actual current distribution in the PCS can differ substantially from that predicted by the classical 'shock wave-magnetic piston' model. In particular, magnetic probe measurements often demonstrate a two-peak PCS structure (see, e.g., [25]). Three-fluid MHD simulations of the Z-pinch PCS [26] have shown that, since the plasma temperature and, accordingly, plasma conductivity in the PCS in the initial stage of the discharge are low, the magnetic field diffuses into the shock wave, which leads to the formation of a current density peak ahead of the shock front. In [27], it was supposed that, in the stage of discharge chamber training (degassing), a significant fraction of the current can flow in the shock wave and the current is redistributed into the magnetic piston only when the facility reaches its standard operating mode. In [28], it was demonstrated by means of synchronized high-speed photography and magnetic probe measurements that, in the standard operating mode, more than 85% of the current flows in the magnetic piston. Thus, the PCS structure depends substantially on the discharge mode. Systematic measurements of the PCS structure, however, have not been performed as yet.

In this paper, we present the result of measurements of the PCS current in the stage close to the instant of pinch formation on the PF-1000 facility [29] operating with deuterium at an energy stored in the capacitor bank of 250–500 kJ. The measurements were performed using absolutely calibrated magnetic probes. The PCS structure was studied using original magneto-optical probes simultaneously recording the dB/dt signal and the plasma optical glow. Along with magneto-optical probes, a Rogowski coil recording the total discharge current and three magnetic probes located inside the PF-1000 collector were also used. The main objective of this paper was to study the dependence of the neutron yield on the total discharge current and the current flowing in the PCS in the final stage of radial plasma compression.

2. Design of magnetic probes and scheme of the experiment

Magnetic probe measurements are widely used to study the dynamics and structure of the PCS in PF discharges [19, 22–25, 27, 28, 30–35]. In most studies, however, this method was used to investigate the PCS behavior in the early stage of the discharge in the regions located far from the pinching zone, because the magnetic probe diagnostics is a contact method and questions always arise concerning the influence of the detector on the plasma characteristics and accuracy of magnetic field measurements. Magnetic probes introduced directly in the pinch formation region may disturb the pinching process. Moreover, intense plasma and radiation fluxes can destroy the probe during one discharge, which substantially complicates experiments.

Taking into account the aforesaid, modified absolutely calibrated magnetic probes for investigating the PCS dynamics under the PF discharge conditions on the PF-1000 facility were designed and manufactured. The new probes were designed on the basis of magnetic probes developed earlier for the experiments carried out on the Angara-5-1 facility [36, 37]. In designing these probes, we took into account many factors limiting the application of magnetic probes in high-power

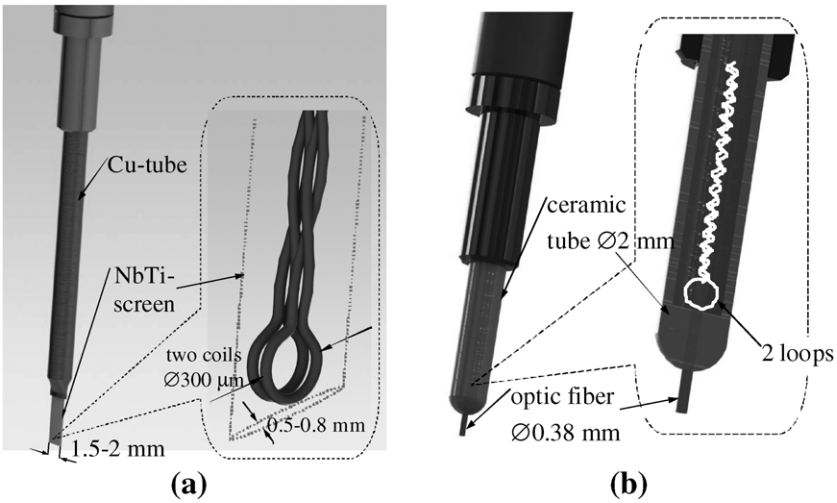

Figure 1. Sensitive elements of (*a*) the plane probe and (*b*) the magneto-optical probe.

discharges, such as the evaporation of the probe case under the action of radiation and particle fluxes, screening of the probe by the plasma, and plasma perturbations arising due to plasma flow around the probe [38]. To improve conditions for plasma flow around the probe and minimize the influence of the probe on the processes under study, the sensitive element of the probe was made planar with a transverse size of 0.7–0.8 mm. Application of such probes on the Angara-5-1 facility for measurements of magnetic fields during the implosion of 20 mm diameter cylindrical wire arrays demonstrated their efficiency [39, 40]. Later on, these probes were successfully adapted to the experimental conditions of the PF-3 plasma focus facility [22–24].

The probes designed for measurements of the azimuthal magnetic field distribution in the stage of PCS compression in the PF-1000 facility consist of two ~300 μm-diameter coils wound in clockwise and counterclockwise directions. The design of the sensitive element of the probe is shown in figure 1(*a*). The coils are packed in a common plane screen made of a niobium-titanium foil with a thickness of 10–15 μm, which is less than the skin depth for the characteristic times of the processes under study. The time of electromagnetic field diffusion through such a screen was calculated in MHD approximation for supersonic plasma flow with a frozen-in magnetic field and for parameters of the Angara 5-1-facility which is closed to parameters of PF-1000: $n_e = 5 \times 10^{17}$–10^{19} cm^{-3}, plasma velocity 10^6–5×10^7 cm s^{-1}, magnetic field 0–100 kG, T = 1–30 eV [37]. For the total size of the sensitive element of the probe in the direction perpendicular to the incident plasma flow 0.7–0.8 mm, the calculated diffusion time is ~1.5 ns. Two symmetric signals of different polarity from two coils allow one to be sure of their magnetic origin. At the instant of probe destruction, the symmetry of the signals violates.

Each probe measured the time derivative of the azimuthal magnetic field $dB_\varphi(r, \varphi)/dt$ at its location. To determine the current flowing within the radius at which the probe was installed, the signal was integrated numerically under the assumption that the plasma current was symmetric with respect to the system axis.

The probes were calibrated using a homogeneous ac magnetic field with a known amplitude and known frequency by the method described in [37]. The probe sensitivity was ~(1.0–5.0) $\times$ 10^{-11} V G^{-1} s^{-1}. The calibration accuracy was better than 5%, and the accuracy in determining the magnetic induction in plasma with account of calibration was about 15–20%.

The PCS structure was studied using specially developed magneto-optical probes. Along with the time derivative of the azimuthal magnetic field, these probes also recorded the plasma optical glow at their location. Similar probes were earlier used to study the process of shock wave formation during the compression of a transverse magnetic field by a supersonic ($M_A > 3$) plasma flow [41, 42]. Later on, such a probe was used to investigate the PCS structure in the early stage of radial plasma compression in the PF-3 facility [43].

The design of the magneto-optical probe is shown in figure 1(*b*). The shape of the sensitive element of the probe was modified: the plane head was replaced by a 2 mm diameter ceramic tube. Two channels for recording the magnetic field were supplemented with a 0.38 mm diameter polymer optical fiber placed in the common case with the magnetic coils. A short segment of the optical fiber (~1 mm) protruded from the protecting ceramic tube into the discharge.

The second end of the optical fiber was connected to a photomultiplier tube (PMT). In processing the recorded signals, all the cable time delays, the propagation time of photons along the optical fiber, and the PMT electron transition time (ETT) were taken into account. The magnetic channels of these probes were also calibrated by the abovementioned method [37].

The experiments were performed on the PF-1000 Mather-type facility. The large-scale PF-1000 facility (figure 2) consists of the following main units:

- The condenser bank and pulsed electrical power circuit with a collector and low-inductance cables.
- The mechanical vacuum and gas system consist of the vacuum chamber, coaxial electrodes and gas handling system.

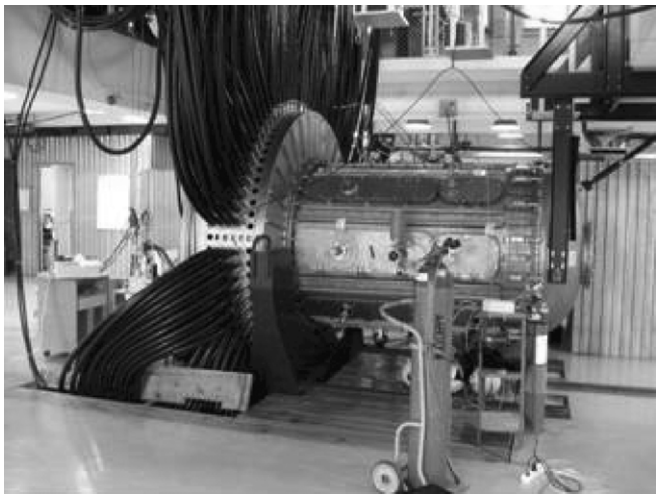

Figure 2. General view of the PF-1000 facility.

The electrical energy is transferred to a collector and electrodes by means of low-inductance cables. The vacuum chamber, which surrounds the electrodes, has a large volume (1400 mm in diameter and 2500 mm in length). Two coaxial electrodes are shown on figure 3. The outer electrode (OE) (cathode) consists of 12 stainless steel rods with 80 mm in diameter. The OE and copper center electrode (CE) radii are 200 mm and 115.5 mm, respectively, with CE length of 460 mm. The cylindrical alumina insulator sits on the CE and the main part of the insulator extends 85 mm along the CE into the vacuum chamber. The insulator prescribes the shape of the initial current sheet between the CE and the back plate of the OE. The condenser bank of capacitance 1332 μF can be charged to voltage ranging between 20 and 40 kV, which corresponded to discharge energies ranging from 266 to 1064 kJ.

During the described experiment, several shots with the PF-1000 upgraded current generator and a new alumina insulator were made.

As was mentioned above, a probe located near the system axis is subject to intense radiation and particle fluxes and, therefore, is destroyed during one shot. Before each subsequent discharge, it is necessary to replace the destroyed probe with a new one. For this purpose, a vacuum lock was created to introduce the probe in the axial region of the system without violating vacuum conditions in the discharge chamber of the facility. This is necessary for the initial discharge conditions (the gas pressure, the concentrations of admixtures in the working gas, etc) to remain unchanged, because the PF discharge is very sensitive to these conditions. The probes were introduced from the collector side through the vacuum lock along the axis of the hollow anode. The system design allowed one to place the sensitive element of the probe near the system axis, namely, near the anode surface at radii of 1.2 and 4 cm and at a distance of 0.5–1.5 cm from the surface of the end flange of the central electrode (anode). The arrangement of the probes in the discharge chamber is shown in figure 3.

It should be noted that, in these experiments, the anode was at a high voltage. In this case, high-voltage breakdown can occur between the anode and the probe, which can lead not only to the probe destruction, but also to a damage of the recording system. To prevent high-voltage breakdowns onto the probe, a measurement scheme was used in which the entire 'probe-oscilloscope' measurement channel was under the anode potential.

In order to monitor the discharge quality, along with magnetic probe measurements, the electrotechnical and emission characteristics of the system were measured in each shot using standard diagnostics applied on the PF-1000 facility. These diagnostics are as follows.

Neutron emission was recorded using four integral activation detectors. The integral neutron yield in these experiments was the main parameter characterizing the discharge quality. In combination with magnetic probe measurements, it allows one to analyze the neutron scaling in terms of the discharge current. Four detectors based on STS-5 and STS-6 counters covered with a silver foil and placed in a neutron moderator were used to increase the measurement accuracy. The detectors were calibrated in their standard positions in the previous PF-1000 experiments.

For time-resolved measurements of radiation we used a scintillator detector (SD) based on PMT with a plastic scintillator installed at a distance of 7 m from the pinch (neutron and hard x-ray radiation) and p–i–n silicon diode covered by filter 10 μm Be and installed at a distance 0.8 m from the pinch (soft x-rays with energy above 600 eV).

The interelectrode voltage was measured by a capacitive divider with a sensitivity of 4 kV/V.

The total discharge current was recorded using a calibrated Rogowski coil with a sensitivity of 470 kA V^{-1}.

The time derivative of the total discharge current was measured using three single-loop magnetic detectors located near the facility collector. The detectors were arranged with a step of 120° along the collector perimeter, which made it possible to estimate the current homogeneity at the collector.

The PCS dynamics and structure were also investigated using a 16-channel laser interferometer with a 1 ns time resolution and a time interval of 10–20 between frames [44].

3. Study of the perturbation arising due to plasma flow around the magnetic probe

The magnetic probe diagnostics of plasma is a contact method, which assumes the plasma impact on the probe and vice versa. In other words, we are dealing with the plasma perturbation introduced by the probe. In this case, the problem of flow around a probe by a magnetized plasma is of primary importance. The accuracy and time resolution of magnetic probe measurements depend on whether the magnetic field has enough time to diffuse from the plasma into the probe case. The situation is especially complicated in the case of supersonic flow around the probe by plasma with a frozen-in magnetic field, accompanied by the formation of a shock wave. The question naturally arises concerning the characteristic scale length and relaxation time of the induced plasma perturbation.

The papers devoted to studying the problem of supersonic flow around bodies of different shapes by a magnetized plasma

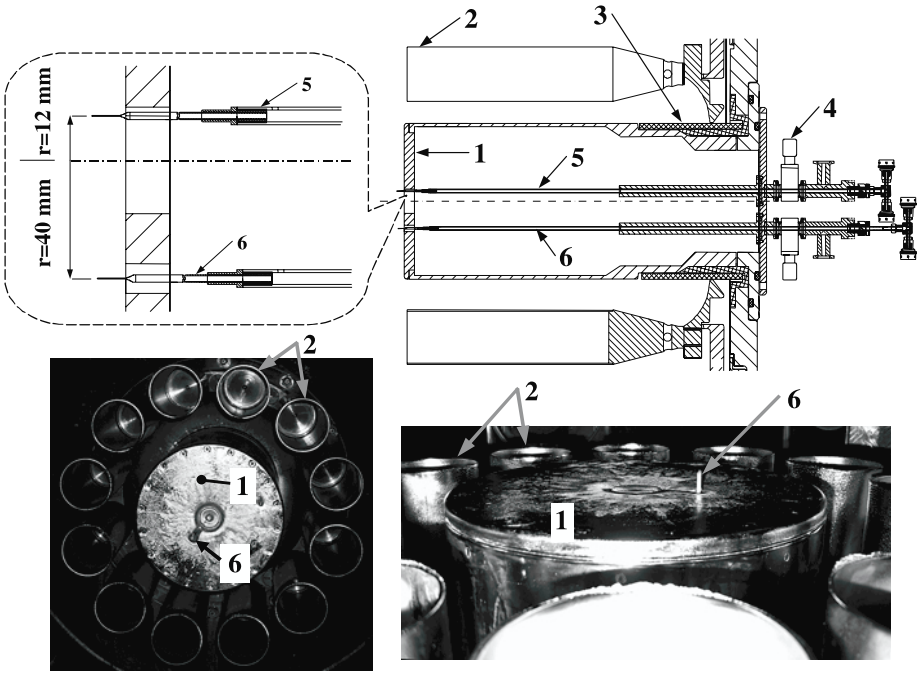

Figure 3. Geometry of the electrodes of the PF-1000 facility and arrangement of the magnetic probes: (1) anode, (2) cathode (12 rods), (3) insulator, (4) vacuum lock though which the probe is introduced, and (5, 6) magnetic probes measuring the azimuthal magnetic field at the radii of 12 mm and 40 mm, respectively. Probe (5) is not shown on the photo.

in high-current discharges are few in number [38, 45, 46]. In our experiments, we used two probe modifications with a plane (0.5×3 mm) case and a cylindrical case (with a diameter of 2.0–2.5 mm). The perturbations introduced by the probes were studied using laser interferometry.

Figures 4 and 5 show interferograms obtained in discharges with a plane probe (shot no 9120) and a cylindrical probe (shot no. 9127) for the same initial conditions (D_2, $P_0 = 1.8$ Torr, $U_0 = 24$ kV and $W_0 = 384$ kJ). Figure 4(a) corresponds to the time at which the PCS passes the probe. After passing the plane probe, the PCS perturbation occupies a narrow region ~1 mm width along the radius (figure 4(b)), and 40 ns later (figure 4(c)), the perturbation completely vanishes.

The plasma perturbation introduced by a cylindrical probe is wider, ~4 mm, which is about 1.6 of the probe size (see figure 5). Although the PCS perturbation in this case is larger than that introduced by the plane probe, it rapidly decays as the PCS propagates toward the system axis. An even larger PCS perturbation is observed in experiments performed with a cylindrical probe at a higher gas pressure ($P_0 = 2.4$ Torr, figure 6). The size of the perturbed region behind the PCS just after it has passed the probe is ~6 mm (figure 6(a)), which is about 2.5 of the initial probe size. After 30 ns, the size of the perturbed region behind the PCS decreases to ~2.5 mm (figure 6(b)) and, after another 40 ns, the perturbation practically vanishes (figure 6(c)). In this case, an unperturbed pinch is observed on the axis (see figure 6(d)).

It should be noted that the radial probe size with account of the projection onto the observation direction is ~3.5–4 mm, which is somewhat larger than the initial probe size. This can be related to the residual PCS plasma and the plasma formed on the probe surface under the action of radiation in the final stage of plasma compression. This plasma can shield the probe and make an appreciable impact on the accuracy of the measurement of the magnetic fields and the degree of this influence strongly depends on the probe shape.

The influence of the plasma flow with a frozen-in magnetic field on the probe signal for probes of different shapes was numerically calculated in [37]. It follows from these calculations that magnetic field perturbations introduced by a plane probe are about 7%. It was found that the measurement error of probes with a plane screen is less than that of probes with a conventional cylindrical screen. For a cylindrical probe, 1 mm in diameter, this error is already 25%. This result was confirmed experimentally on the Angara-5-1 facility [37].

It is natural to assume that the error increases with the increase in the probe size. We have undertaken comparative studies of probes of a different configurations on the PF-1000 facility. In figure 7 the result of current measurements with the different probes obtained in the discharges with practically the same value of the total discharge current and the neutron output is shown. One can see that the current measured with the cylindrical probe is essentially less. The typical value of current amplitude understating under our conditions makes ~1.75. The measurement error decreases during the pulse and at the certain instant, the indications of two probes start to coincide. It is caused by the gradual disintegration of the plasma surrounding a probe, and shielding reduction. It should be noted that, in similar experiments on the FF-3 facility [43], such a strong influence of the probe dimension on the accuracy of measurements was not revealed. Apparently, it is caused by the strong influence of the parameters of the plasma surrounding the probe: the measurements on the PF-3 were done on the large distances from the axis under conditions of less dense and less hot plasma.

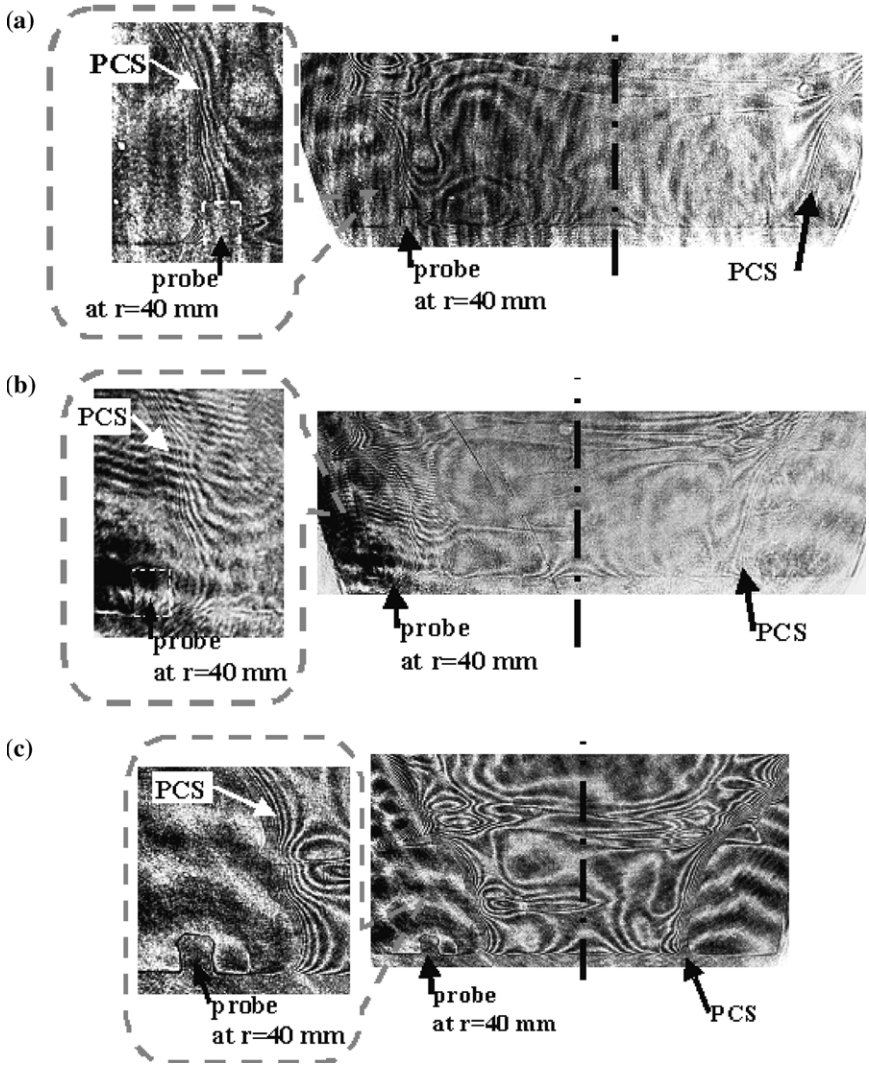

Figure 4. PCS interferograms recorded near the system axis in shot no 9120 (D_2, $P_0 = 1.8$ Torr, $U_0 = 24$ kV and $W_0 = 384$ kJ) with plane probe at different instants from the beginning of the discharge: (*a*) 5824, (*b*) 5844 and (*c*) 5884 ns. The neutron yield is $Y_n \sim 1.3 \times 10^{11}$ neutrons/shot.

The following important conclusions can be drawn from these results:

(i) In the case of a plane probe, the PCS perturbation is much smaller than in the case of a cylindrical probe. It is necessary to take into account at performing the quantitative measurements.
(ii) In spite of a relatively large plasma perturbation introduced by a cylindrical probe, it rapidly relaxes as the PCS propagates toward the axis, so that no perturbation introduced by the probe is observed near the axis.
(iii) The probe parameters do not render an essential influence on its time characteristics. It allows using the probes of the cylindrical form, for example, the magneto-optical probes described above, for studies of the PCS structure.

4. Experimental results

4.1. Study of the azimuthal magnetic field

The dynamics of the azimuthal magnetic field during PCS radial compression was investigated in four experimental sessions with different initial conditions. Taking into account that the number of shots was limited by the number of available probes, the first experiments were performed in a well-reproducible mode with deuterium at an initial pressure of $P_0 = 3$ Torr and a discharge voltage of $U_0 = 27$ kV. In these experiments, the stored energy was about 485 kJ. Before each shot with the magnetic probe, a series of training discharges under standard conditions were performed until the neutron yield became higher than 10^{10} neutrons/shot. Since the probes were destroyed in each shot, the working gas in the chamber was usually refreshed before the next experiment.

Figure 8 shows the results of measurements with a magnetic probe located at a distance of 4 cm from the system axis in a discharge with a high neutron yield. In this discharge, the neutron yield was 1.24×10^{11} neutrons/shot, which is one of the best results obtained in this experimental session. Thus, it can be asserted that, in the given experimental scheme, the probe located in the PCS compression region at a distance of 4 cm from the axis insignificantly affects the pinching process and, accordingly, the neutron yield. It follows from figure 8(*a*)

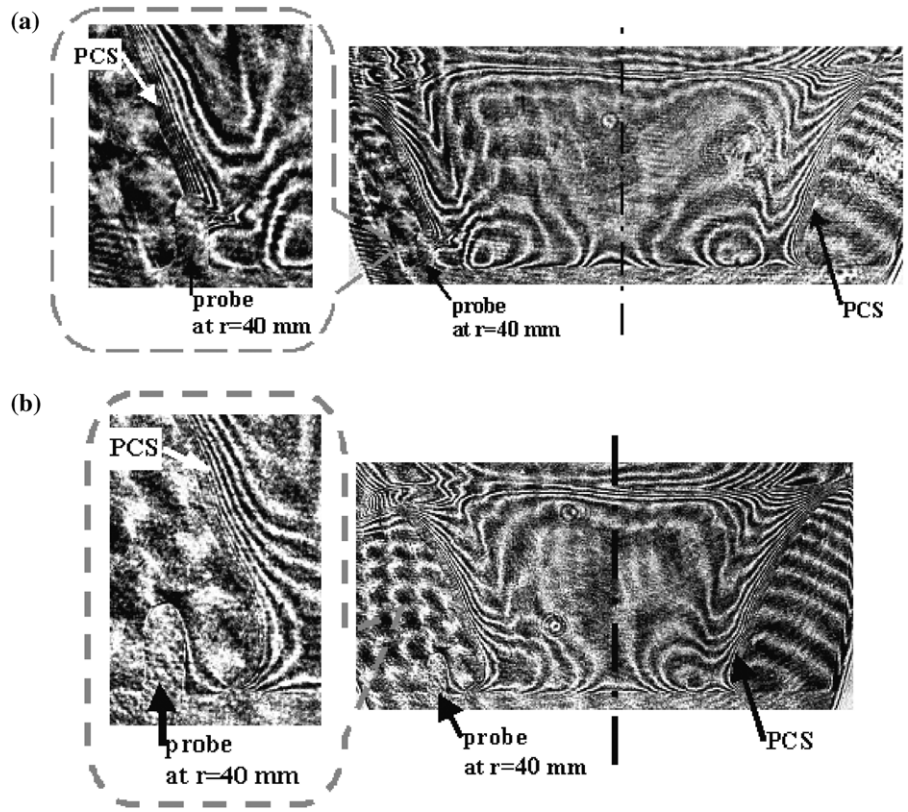

Figure 5. PCS interferograms recorded near the system axis in shot no 9127 (D_2, $P_0 = 1.8$ Torr, $U_0 = 24$ kV and $W_0 = 384$ kJ) with cylindrical probe at different instants from the beginning of the discharge: (*a*) 5793 and (*b*) 5913 ns. The neutron yield is $Y_n \sim 1.7 \times 10^{11}$ neutrons/shot.

that the signal from the magnetic probe appears about 6.2 μs after the beginning of the discharge. As a rule, it has one or two maxima, which indicates that the current distribution in the PCS is rather complicated. In particular, in this shot two peaks were recorded, the full width at half-maximum (FWHM) of each peak being ~35–40 ns. A precursor in the form of a small-amplitude pulse before the main signal was also observed. The presence of such a precursor, which can carry ~5–7% of the total PCS current, is typical of many our discharges and its origin is unclear.

The signals from two different probe coils remain practically symmetric over ~200 ns, which confirms their magnetic nature. Later on, the symmetry of these signals is abruptly violated (see the vertical dashed line in figure 8(*a*)), which indicates that at least one coil is destroyed. After this instant, the signals were not processed. However, even this time interval is quite sufficient to determine the current flowing in the PCS. This current was recovered under the assumption that the PCS was axisymmetric.

It can be seen that, over ~100 ns, the PCS current reaches its maximum value of ~1.7 MA, which corresponds, to within measurement errors, to the total discharge current measured by the Rogowski coil or recovered using the signals from the loop detectors measuring the time derivative of the total current. A certain difference in the signals from of the loop detectors can be caused by the inhomogeneous current distribution at the collector, because the loop detectors are arranged with a step of 120° along the collector perimeter. A more abrupt drop in the signal from the Rogowski coil at the instant of dip (a peak in the time derivative of the total current) can be attributed to the partial differentiation of this signal.

Under the conditions in which the total discharge current varies insignificantly while the PCS passes the probe, the signal maximum corresponds to the instant at which the entire PCS current begins to flow inside the 4 cm radius region. After this, until the probe is destroyed, the behavior of the current measured by the probe coincides with that of the total current, i.e. the measured current decreases in accordance with the reduction in the total discharge current. An important consequence of this result is that the discharge current is efficiently compressed toward the axis (at least to a radius of 4 cm), which results in the high value of neutron yield in this discharge.

At the instant of dip (at the peak of the total current derivative), an abrupt increase in the voltage up to 50 kV is observed in the voltage waveform.

Figure 9 shows the results of similar measurements performed with the use of two magnetic probes, one of which was installed at a distance of 12 mm from the axis.

The signal from the magnetic probe located at the radius of 40 mm also appears about 6.2 μs after the beginning of the discharge, whereas the signal from the probe located at the radius of 12 mm appears 130 ns later. From the time delay between these signals, we find that the average PCS radial velocity between these probes is $\approx 2.1 \times 10^7$ cm s^{-1}. For this

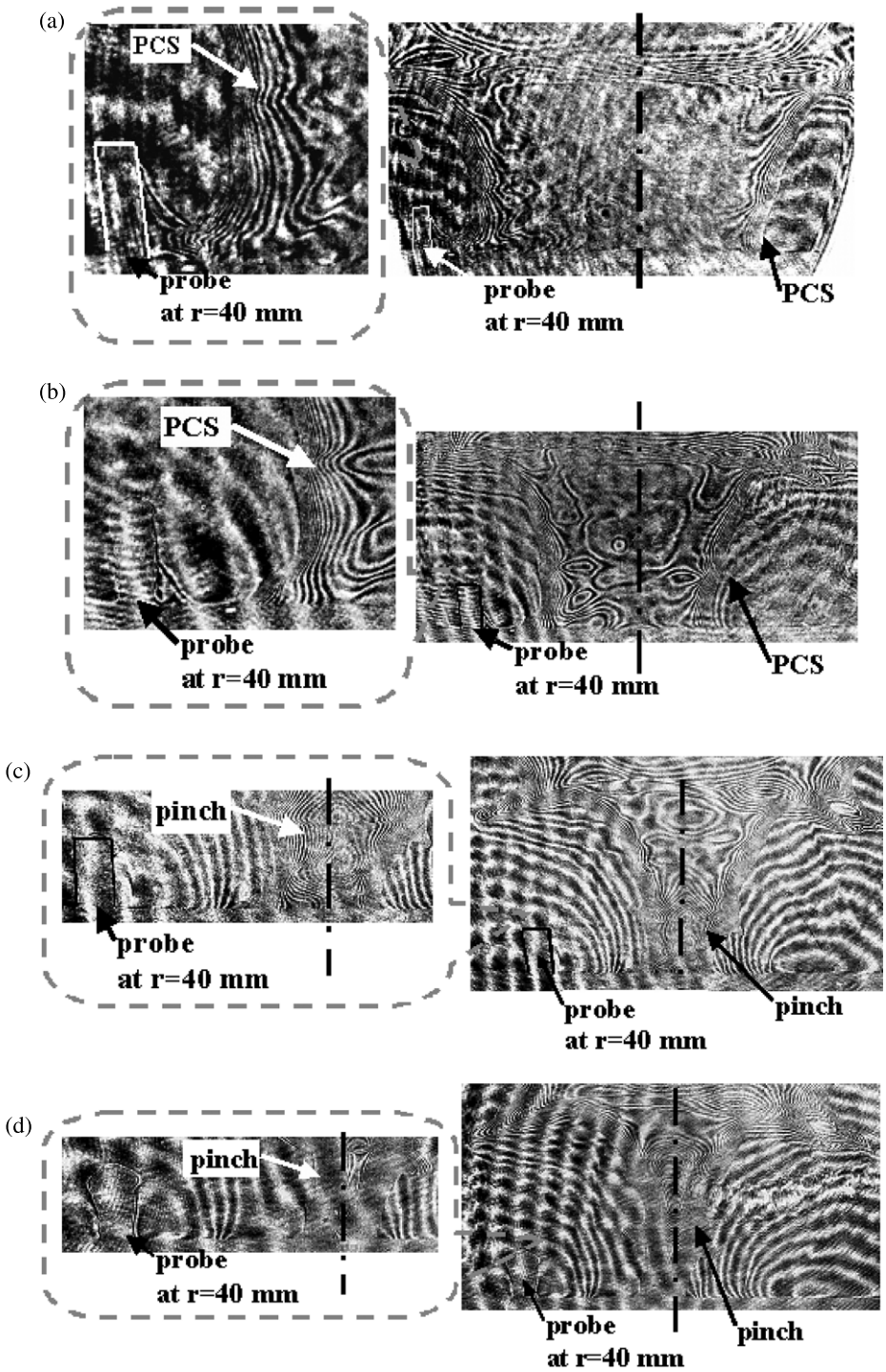

Figure 6. PCS interferograms recorded near the system axis in shot no 9131 (D_2, $P_0 = 2.4$ Torr, $U_0 = 24$ kV and $W_0 = 384$ kJ) with cylindrical probe at different instants from the beginning of the discharge: (*a*) 6479, (*b*) 6509, (*c*) 6549 and (*d*) 6569 ns. The neutron yield is $Y_n \sim 8.7 \times 10^{10}$ neutrons/shot.

velocity, the skin depth estimated from the formula

$$\dot{I} \approx I \times \left(\frac{V_r}{\delta_{\text{skin}}}\right)$$

is $\delta_{\text{skin}} \approx 1.6$ cm. Under the assumption of the Spitzer conductivity, this value corresponds to the plasma electron temperature of $T_e \approx 50$ eV. Discharge current somewhat increases (to 1.9 MA in our case); however, the fraction of the current compressed to the axis decreases substantially, which resulted in a reduction in the neutron yield. In this discharge, the discharge current was also almost completely compressed to the radius of 4 cm, but the neutron yield was about one-half order of magnitude lower than in the above discharge. Unfortunately, the probe installed at the radius of 12 mm was destroyed very soon; therefore, it was impossible to measure the current amplitude in this region. It is natural to assume that the probe installed so close to the axis could affect the process of pinch formation. This conclusion, however,

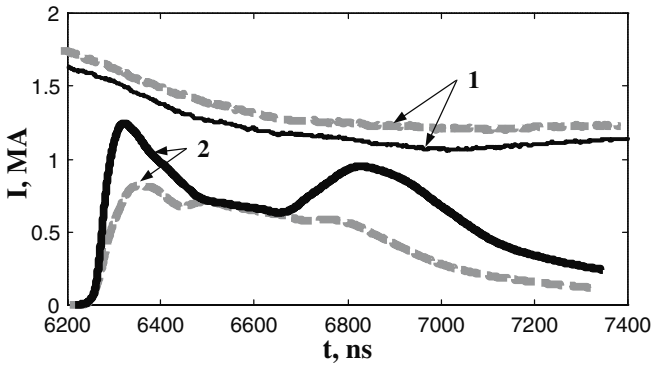

Figure 7. Total discharge current (1) and current recovered from the probe measurement (2) obtained under the same initial conditions (D_2, $P_0 = 1.8$ Torr, $U_0 = 24$ kV and $W_0 = 384$ kJ) by the plane probe (solid line, shot 9341, $Y_n = 6.9 \times 10^{10}$ n/pulse) and by the cylindrical probe (dashed line, shot 9340, $Y_n = 9.8 \times 10^{10}$ n/pulse). Probe location is 4 cm from the discharge system axis.

can occur too hastily. First, earlier experiments carried out on the PF-3 facility with the use of x-ray pinhole cameras and frame cameras [22, 24, 43] demonstrated that a similar probe located at a distance of 2 cm from the system axis practically did not affect the process of pinch formation. On the other hand, the lower neutron yield in this discharge can be explained by other factors, in particular, a lower PCS current (~1.5 MA) and a broader PCS with a complicated structure. The neutron yield measured in this discharge lies within the admissible scatter observed in a series of reference experiments performed without magnetic probes. Nevertheless, taking into account fast destruction of the probe located so close to the axis and, accordingly, the impossibility of obtaining reliable information on the PCS parameters at this radius, we abandoned the application of such probes at this position.

Another experimental session was performed after the power supply of the PF-1000 facility was upgraded. This made it possible to attain discharge currents of 1.5–1.9 MA at a lower bank voltage of 20–24 kV, which corresponds to a lower discharge energy, $W = 260$–380 kJ. However, although the energy deposited in the discharge was lower than in the previous series of experiments, the neutron yield remained at the same level of 10^{10}–10^{11} neutrons/shot. This indicates the conditional character of the energy scaling and the importance of the current scaling.

This fact was clearly demonstrated in our experiments. In particular, we performed measurements in the stage of discharge system training, during which the discharge voltage was gradually increased. In the course of training, the neutron yield gradually increased with increasing discharge voltage from 20 to 23 kV (figures 10(*a*) and (*b*)). However, when the voltage increased to 24 kV, the neutron yield degraded abruptly. Probe measurements showed that, in this case, the efficiency of current transportation toward the axis decreased substantially.

The probe located at the radius of 40 mm recorded only about one-half of the total current measured by the Rogowski coil (figure 10(*c*)). It should be noted that, along with the upgrade of the power supply, the insulator of the discharge system was also replaced. It is well known that, in this case, it is necessary to gradually train the discharge system in order

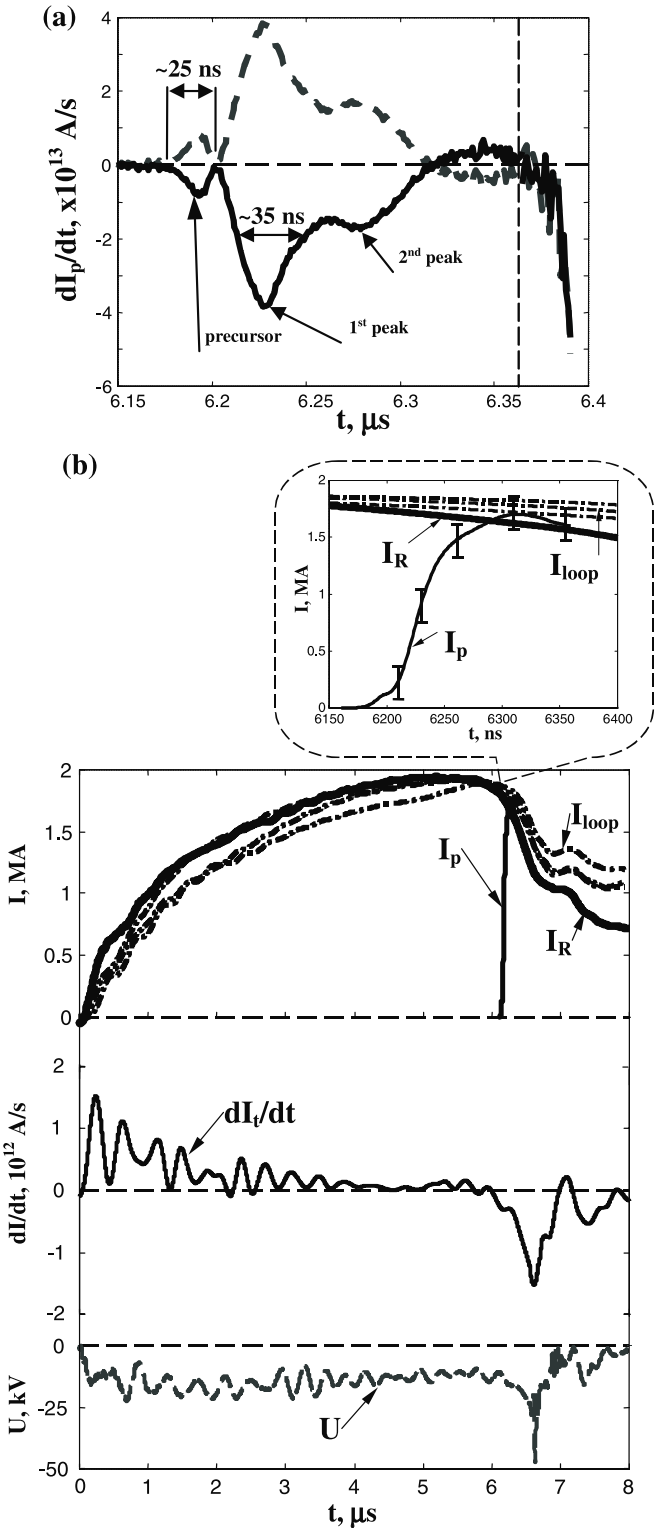

Figure 8. Results of the measurement of the azimuthal magnetic field in shot no 8220 (D_2, $P_0 = 3$ Torr, $U = 27$ kV and $W = 485$ kJ): (*a*) current time derivatives measured by the two coils of the probe (the vertical dashed line shows the instant of probe destruction) and (*b*) current measured by the magnetic probe (I_p), total discharge current measured by the integrating Rogowski coil (I_R), total discharge current measured by the loop detectors at the collector (I_{loop}), time derivative of the total discharge current $(dI/dt)_t$ and voltage (U). The probe is at $R = 40$ mm and $Z = 10$ mm. The neutron yield is 1.24×10^{11} neutrons/shot.

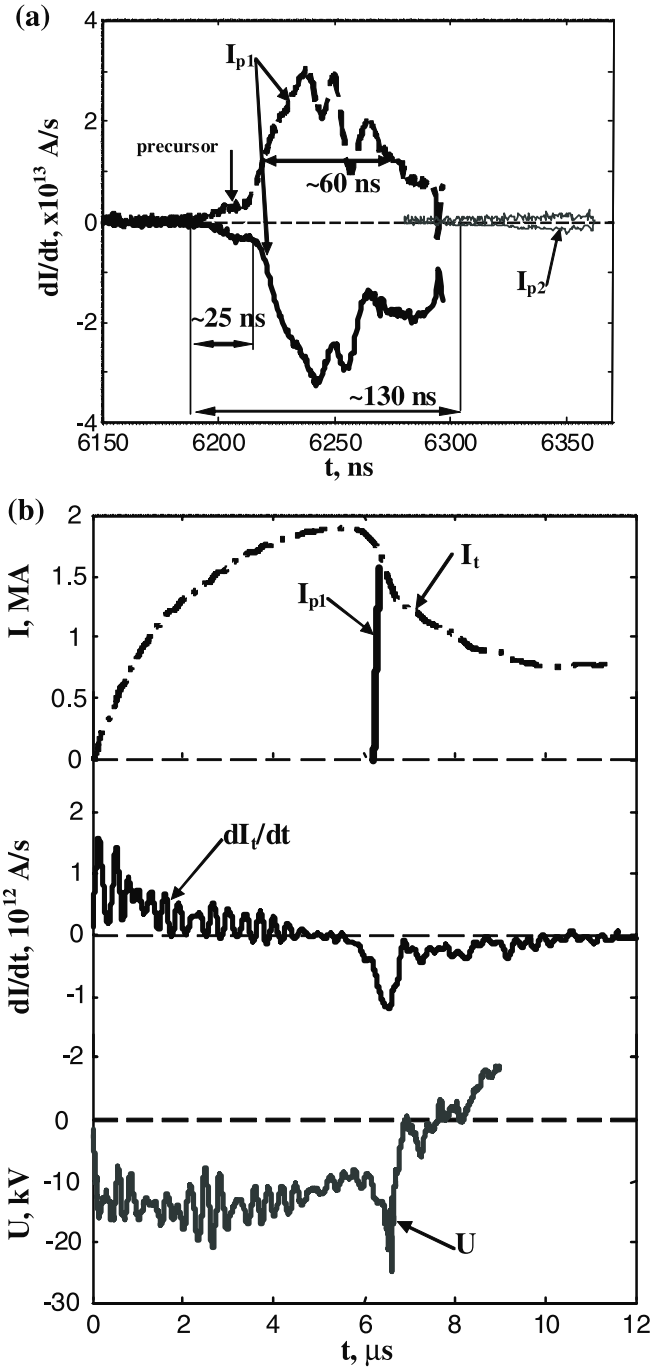

Figure 9. Results of the measurement of the azimuthal magnetic fields in shot no 8211 (D_2, $P_0 = 3$ Torr, $U = 27$ kV and $W = 485$ kJ): (*a*) current time derivatives measured by the probes installed radially at $R = 40$ mm, and axially at $Z = 15$ mm (P1) and $R = 12$ mm, $Z = 20$ mm (P2) and (*b*) current measured by the magnetic probe installed at $R = 40$ mm (I_{p1}), total discharge current I_t, time derivative of the total discharge current $(dI/dt)_t$ and voltage (U). The neutron yield is 2.6×10^{10} neutrons/shot.

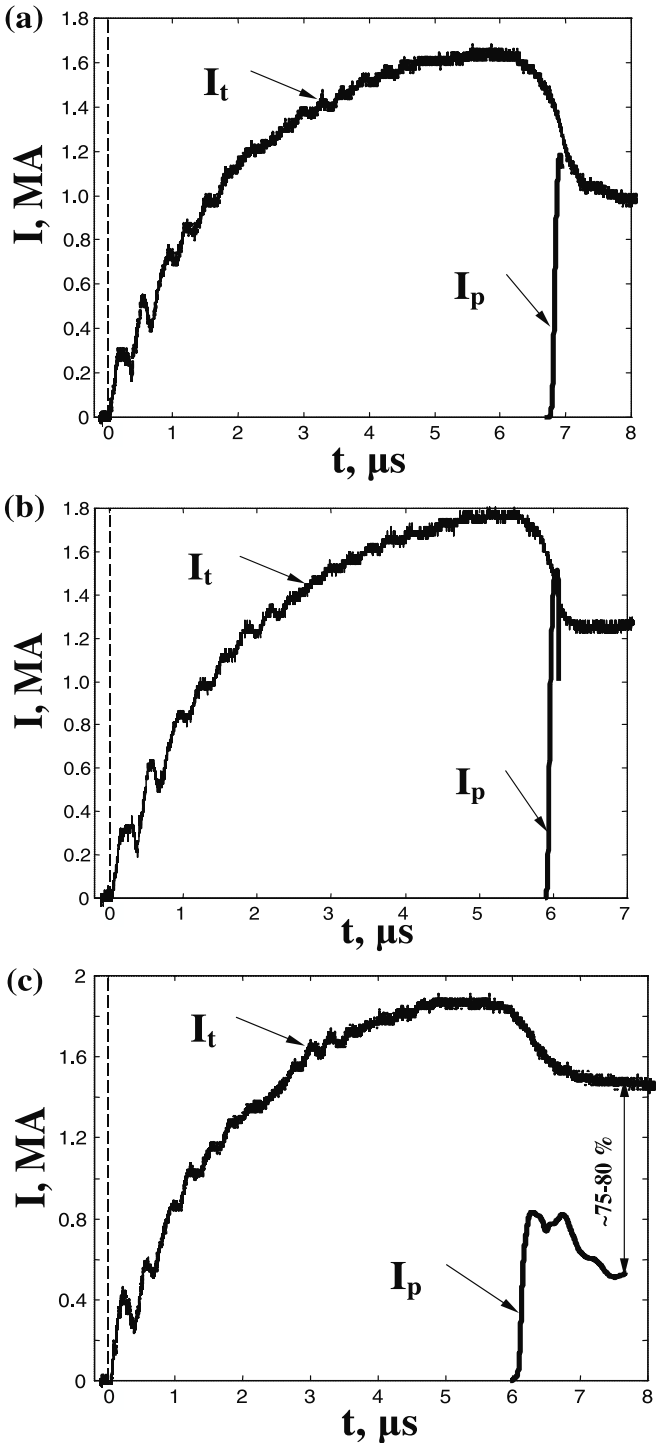

Figure 10. Results of measurements of the azimuthal magnetic fields (D_2, $P_0 = 2$ Torr) at different discharge voltages: (*a*) shot 8465, $U_0 = 20$ kV, $W_0 = 266$ kJ and $Y_n = 5.1 \times 10^9$ neutrons/shot; (*b*) shot 8479, $U_0 = 23$ kV, $W_0 = 352$ kJ and $Y_n = 1.0 \times 10^{11}$ neutron/shot; and (*c*) shot 8466, $U_0 = 24$ kV, $W_0 = 383$ kJ and $Y_n = 1.5 \times 10^8$ neutrons/shot.

to degas its elements. Apparently, for a discharge voltage of 24 kV, gas release from the insulator was so intense that it led to secondary breakdowns along the insulator [23]. Due to the shunting of the main current channel, the total discharge current somewhat increases (to 1.9 MA in our case); however, the fraction of the current compressed to the axis decreases substantially, which resulted in a reduction in the neutron yield.

4.2. Study of the PCS structure

The PCS structure was studied using the magneto-optical probe described above. The probe was introduced in the

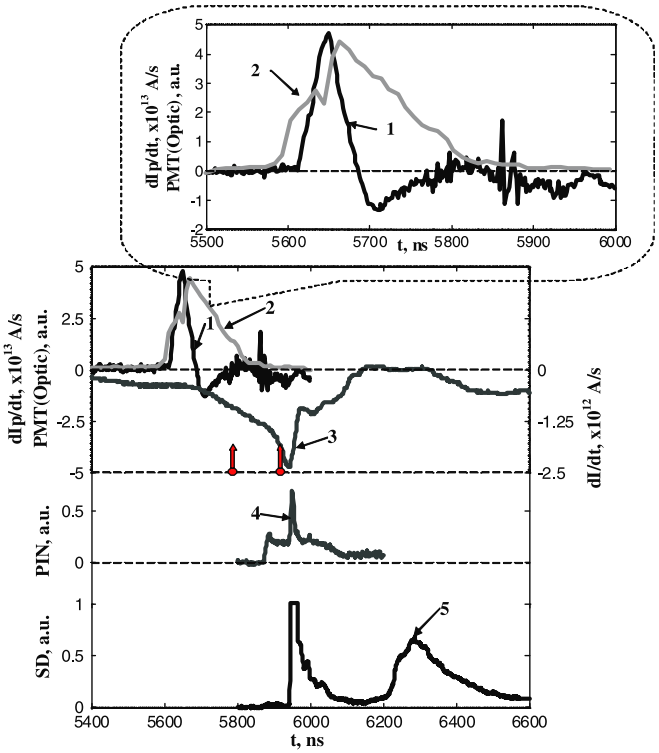

Figure 11. Results of measurements of the PCS structure by the magneto-optical probe (shot 9127), D_2, $P_0 = 1.8$ Torr, $U_0 = 24$ kV and $W_0 = 384$ kJ). (1) Current time derivative measured by the magnetic probe installed at the radius of 40 mm, (2) PMT signal, (3) time derivative of the total current measured by the loop detector at the collector, (4) signal from pin-diode (PIN) and (5) signal from the scintillator detector (SD). The upward arrows indicate the instants corresponding to the laser interferometry frames in figure 5. The neutron yield is $Y_n \sim 1.7 \times 10^{11}$ neutrons/shot.

discharge through an anode aperture at a distance of 4 cm from the system axis (figure 3). Therefore, unlike [43], the PCS structure in the stage of its well-developed radial compression was investigated. The experiments were performed on the upgraded PF-1000 facility after reaching the optimal operating mode at $V = 24$ kV ($W = 383$ kV) and a deuterium pressure of 1.8–2.4 Torr.

Figure 11 shows the signals from the magnetic (1) and optical (2) channels of the magneto-optical probe. It should be noted that these results were obtained in a well-reproducible regime with a voltage of 24 kV. In contrast to the results presented in figure 10(*c*), the current recorded in this discharge by the probe located at the radius of 4 cm coincided with the total discharge current and reached 1.8 MA (taking into account the correction factor 1.75 as it was shown above in part 3). Accordingly, the neutron yield in this discharge was as high as 1.7×10^{11} neutrons/shot.

Figure 11 also shows the signals from the SD located at 7 m side-on and from p–i–n detector. P–i–n detector registered the signal of SXR radiation, SD registered the hard x-ray, which appears close to the dip on the current derivative (taking into account the time of flight of photons) and neutrons, delayed in correspondence with the time of flight of neutrons with energy ~2.45 MeV. The time correlation of radiation on the PF-1000 facility was discussed in more detail in [47].

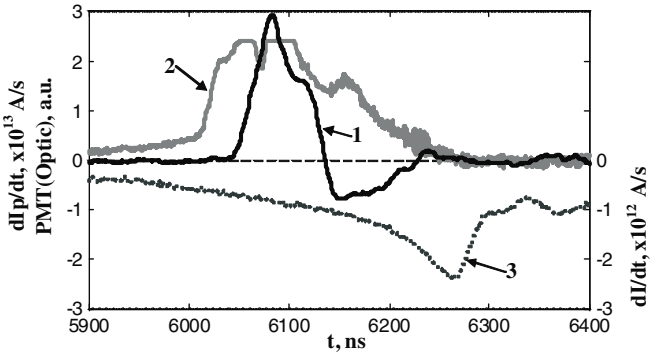

Figure 12. Results of measurements of the PCS structure by the magneto-optical probe (shot 9143, D_2, $P_0 = 2.1$ Torr, $U_0 = 24$ kV and $W_0 = 384$ kJ). (1) Current time derivative measured by the magnetic probe installed at the radius of 40 mm, (2) PMT signal, (3) time derivative of the total current measured by the loop detector at the collector. The neutron yield is $Y_n \sim 8.6 \times 10^{10}$ neutrons/shot.

It should be noted that the probe with such a design survives much longer. The probe is again destroyed in every discharge, but at a much later time. This allows us to trace the current dynamics inside the radius of 40 mm until the formation of the pinch and its subsequent decay.

It follows from figure 11 that the optical signal from the magneto-optical probe (PMT signal) has a steep front and appears about 30 ns before the magnetic signal. The signal has a double-humped structure.

The first maximum is reached ~50 ns after the beginning of the signal, after which the signal decreases and then increases again. Then, the signal gradually relaxes to zero and, at the instant of pinch formation on the axis, it practically vanishes. The first peak can be interpreted as the formation of a shock wave at the front of the magnetic piston. This shock wave snowplows and ionizes the neutral gas filling the discharge chamber. The plasma optical glow depends on many parameters (e.g. density and temperature of plasma, the type of working gas), and the most intensely glowing region does not always correspond to the maximum plasma density and/or temperature. But between the neutral undisturbed gas and the magnetic piston, the intensively radiated region with relatively cold and dense plasma surely exists. Namely this region we interpret as a leading edge of SW. We associate this edge with the 'umbrella'-like images of PCS detected by various visible cameras (see, for example, [28]). Optical aperture of the magnetic probe allows us to estimate the instant of SW passing through the probe and study the time correlation between SW and magnetic piston. The second peak is probably related to the deceleration of a fraction of the plasma and its accumulation on the probe case. After passing through the PCS, this plasma gradually cools down and decays in such a way that the perturbation introduced by the probe vanishes over a rather short time. It corresponds to the perturbations decay observed on the interferograms (see section 3).

Figure 12 shows similar results obtained at a higher gas pressure. When comparing signals from the optical probes in different discharges, it should be taken into account that, the optical output was not calibrated; therefore, the intensities of the PCS glow in different discharges cannot

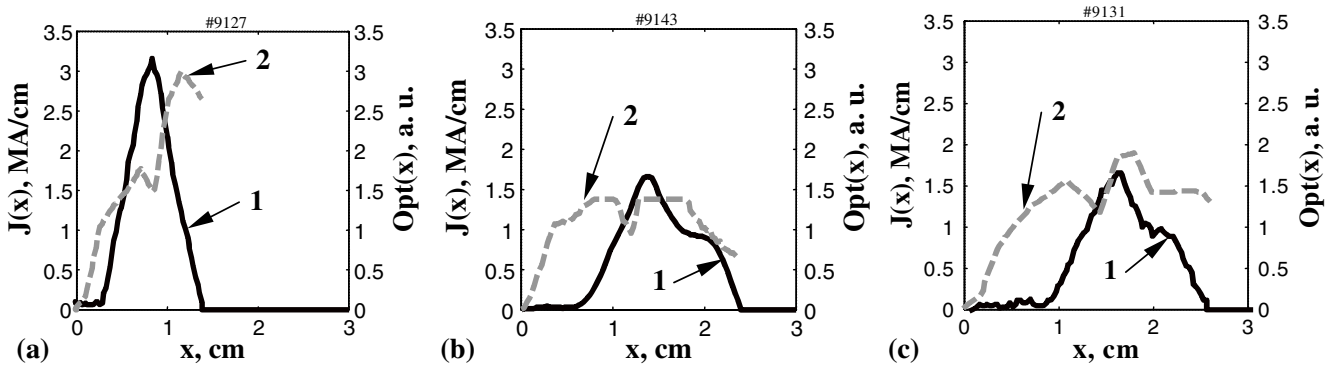

Figure 13. Distributions of the (1) linear current density and (2) plasma optical glow across the PCS (D_2, $U_0 = 24$ kV and $W_0 = 384$ kJ) at different gas pressures: $P_0 =$ (*a*) 1.8, (*b*) 2.1 and (*c*) 2.4 Torr. The neutron yields are $Y_n \sim 1.7 \times 10^{11}$, 8.6×10^{10} and 8.7×10^{10} neutrons/shot, respectively.

be compared. Nevertheless, these results allow us to draw important conclusions on the dynamics and structure of the PCS. It is seen that even a slight increase in the pressure results in the shift of both the instant at which the PCS arrives at the probe and the instant of pinch formation by 300–500 ns. The optical signal appears long before the magnetic signal. Probably, since the probe was not collimated, it began to record the PCS glow immediately after the PCS reached the anode edge, i.e. during the entire stage of PCS radial compression. This fact manifests itself in the gradual growth of the signal as the PCS approaches the probe. The instant at which the PCS reaches the probe corresponds to the steep front of the signal. This is the instant at which the shock wave arrives at the probe.

5. Discussion of results and neutron scaling

Application of the magneto-optical probe made it possible to study the structure of the PCS in a PF discharge on the PF-1000 facility. It should be noted that, in this stage of the discharge, the shock wave and the magnetic piston are well separated. Since the discharge current varies insignificantly as the PCS passes the probe, it can be stated that, in the first approximation, variations of the magnetic signal are determined by the character of the current distribution inside the PCS and the PCS propagation velocity. The PCS velocity in the final stage of plasma compression can be roughly estimated from the shift between the signal from the magnetic probe and the peak in the time derivative of the total current. For different discharges, this velocity varies in the range $(1.5–2.2) \times 10^7$ cm s^{-1}. Figure 13 shows the distributions of the current density and plasma glow over the PCS thickness obtained for three typical discharges with account of the above assumptions.

Analysis of these distributions allows us to draw the following conclusions. First of all, the PCS in the final stage of plasma compression is rather compact. At low gas pressures, the FWHM of the magnetic piston is as small as 0.5 cm and its full width is about 1 cm. Apparently, these are upper estimates, because the average propagation velocity of the PCS from the probe to the axis used in our estimates can be higher than the PCS velocity near the probe.

As the pressure increases, the width of the magnetic piston increases by nearly a factor of 2, while the total current is preserved. This naturally leads to a decrease in the linear current density in the PCS. However, this insignificantly affects the neutron yield. Finally, if we assume that the thickness of the shock front is determined by the front duration of the light signal, whereas the subsequent glow is caused by the plasma surrounding the probe, then we find that the width of the shock front also increases from several millimeters at a low pressure to ~1 cm at higher pressures. An important consequence of these estimates is that most of the current flows in the magnetic piston. For example, in figure 13(*c*), the magnetic signal appears after the optical signal has reached its maximum value, i.e. only a few percent of the PCS current flows in the shock wave. Thus, it can be stated that a compact high-quality PCS forms in the standard operating mode of the PF-1000 facility in the final stage of plasma compression and that the dynamics and structure of the PCS are well described by the snowplow model. In this case, the gas snowplowing efficiency is fairly high and, accordingly, the leakage currents are low. It should be noted that, in all of the above discharges, the current measured by the probe coincided with the total discharge current and the neutron yield was high.

The above considerations clearly demonstrate the problem of the efficiency of discharge current transportation toward the axis. Figure 14 shows the measured neutron yield as a function of the current measured by a probe installed at a radial distance of 40 mm from the axis (figure 14(*a*) and of the total current measured by the Rogowski coil and loop detectors at the instant at which the PCS passes the probe (figure 14(*b*)).

It is seen that the known neutron scaling agrees well with the data obtained using the magnetic probe. At the same time, the neutron yield is practically independent of the total discharge current. Obviously, the high neutron yields in figure 14(*b*) correspond to the high efficiency of current compression onto the axis, as is observed, e.g., in figure 8. It should be noted that, in some discharges, the neutron yield is very low in spite of the high value of the total discharge current. This fact is related to secondary shunting breakdowns, due to which only a lower fraction of the total current contributes to the pinch formation (figure 10(*c*)).

Unfortunately, we could not measure the current at closer distances to the axis because of the fast destruction of the

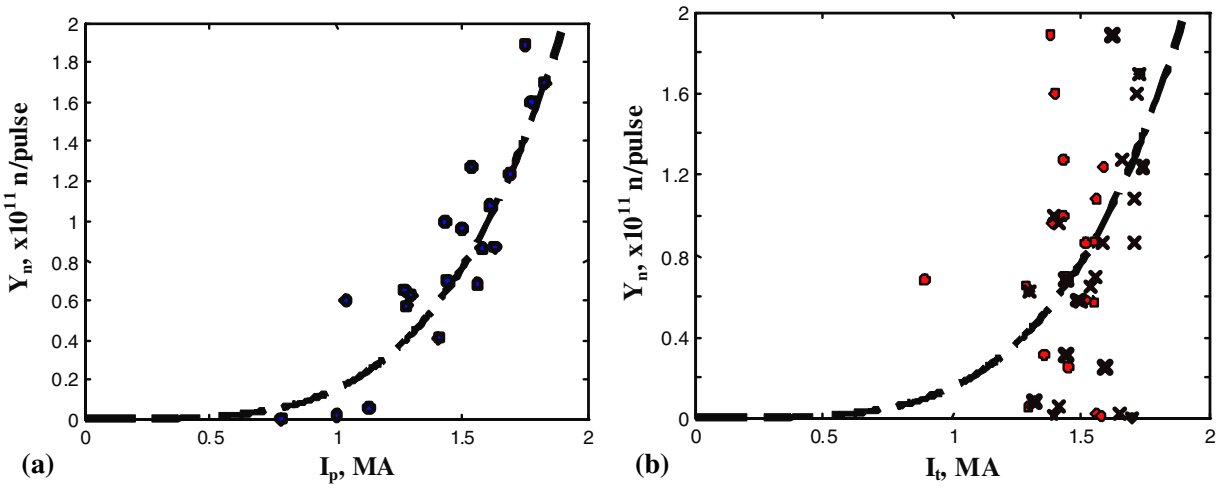

Figure 14. Neutron yield Y_n as a function of (*a*) the maximum current recorded by the magnetic probe at the radius of 40 mm and (*b*) the current measured by the Rogowski coil (●) and loop detectors (×) at the instant at which the PCS passes the probe. The dashed line shows the scaling $Y_n = 1.5 \times 10^{10} I^4$, where I is the current (in MA).

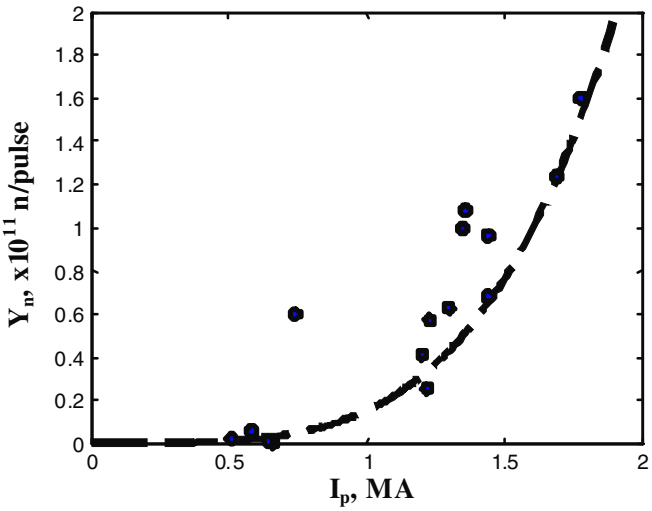

Figure 15. Neutron yield Y_n as a function of the current recorded by the magnetic probe at the radius of 40 mm at the instant of dip. The dashed line shows the scaling $Y_n = 1.5 \times 10^{10} I^4$, where I is the current (in MA).

probe installed at the radius of 12 mm. Nevertheless, analysis of oscillograms shows that, when the current is efficiently compressed onto the axis, the behavior of the signal from the probe installed at the radius of 40 mm agrees well with that of the total discharge current. Figure 15 shows the neutron yield as a function of the current measured by the magnetic probe at the instant of dip. It can be seen that, at least for the probes that are still undestroyed, the shape of this dependence remains generally the same.

6. Conclusions

The application of absolutely calibrated magnetic probes of different design on the PF-1000 facility made it possible to obtain new data on the parameters and dynamics of the PCS of the PF discharge at high values of the energy deposited in the discharge.

It is shown that a compact high-quality PCS forms in the final stage of plasma compression and that the dynamics and structure of the PCS are well described by the snowplow model, according to which a shock wave that efficiently ionizes and snowplows the neutral gas forms in front of the magnetic piston. The total PCS thickness is in the range 1–2 cm, depending on the working gas pressure. In this case, most of the current flows in the magnetic piston.

The current flowing in the PCS in the final stage of radial plasma compression at a distance of 40 mm from the system axis was measured. In the optimal operating modes, this current is equal to the total discharge current (with uncertainty of 20%), which indicates the high efficiency of current transportation toward the axis. At the same time, if the snowplow mechanism is violated and shunting currents appear, which is especially pronounced in the stage of training of the discharge system, less than 50% of the total discharge current can be compressed onto the axis.

It is shown that the neutron yield is determined just by the current compressed onto the axis. The dependence of the neutron yield on this current agrees well with the known scaling, $Y_n \sim I^4$. The use of the total discharge current in constructing the current scaling, especially for facilities with a large stored energy, is unjustified.

It is demonstrated with the help of laser interferometry, that plasma perturbations introduced by probes with the given design are relatively small and practically do not affect the process of pinch formation.

Acknowledgments

This work was supported in part by the Russian Foundation for Basic Research (project nos. 10-02-00449-a, 10-08-00287-a and 11-02-01212-a) and by the research program no LA08024 of the Ministry of Education, Youth and Sport of the Czech Republic.

References

[1] Rager J P 1981 The Plasma Focus *Com. Naz. Energ. Nucl. Centr. Frascati (Pap.)* 81.19/cc
[2] Bernard A *et al* 1998 *J. Moscow Phys. Soc.* **8** 93
[3] Pouzo J 1999 *Proc. 2nd Symp. on Current Trends in Int. Fusion Research (Washington, DC, 1997)* ed E Panarella (Ottawa: NRC Research Press 41654) p 41
[4] Maisonnier Ch, Samuelli M, Robouch B and Pecorella F 1970 *Proc. 4th European Conf. on Controlled Fusion and Plasma Physics (Rome, Italy, 1970)* C.N.E.N. Roma p 117
[5] Filippov N V *et al* 1971 *Proc. 4th Int. Conf. on Plasma Physics and Controlled Nuclear Fusion Research (Madison, WI,1971)* ed R Schenin and J W Well (Vienna: IAEA) vol I pp 573–600
[6] Rapp H 1973 *Phys. Lett.* A **43** 420–2
[7] Michel L, Schonbach K H and Fisher H 1974 *Appl. Phys. Lett.* **24** 57–9
[8] Soto L 2005 *Plasma Phys. Control. Fusion* **47** A361–81
[9] Soto L, Pavez C, Tarifeño A, Moreno J, and Veloso F 2010 *Plasma Sources Sci. Technol* **19** 055017
[10] Gourlan C, Kroegler H, Maisonnier Ch, Rager J P, Robouch B V and Gentilini A 1979 *Proc. 7th Int. Conf. on Plasma Physics and Controlled Nuclear Fusion Research (Innsbruck, Austria 1978)* vol II (Vienna: IAEA) pp 123–34
[11] Herold H, Jerzykiewicz A, Sadowski M and Schmidt H 1989 *Nucl. Fusion* **29** 1255–66
[12] Sadowski M J and Scholz M 2002 *Nukleonika* **47** 115–55
[13] Krauz V I 2006 *Plasma Phys. Control. Fusion* **48** B221–9
[14] Coverdale C A *et al* 2007 *Phys. Plasmas* **14** 022706
[15] Nukulin V Ya and Polukhin S N 2007 *Plasma Phys. Rep.* **33** 271–7
[16] Lee S 2008 *Plasma Phys. Control. Fusion* **50** 105005
[17] Lee S and Saw S H 2008 *J. Fusion Energy* **27** 292–5
[18] Lee S and Saw S H 2008 *Appl. Phys. Lett.* **92** 021503
[19] Gourlan C, Kroegler H, Maisonnier Ch, Oppenländer T and Rager J P 1977 *Proc. 8th European Conf. on Controlled Fusion and Plasma Physics (Prague, Czech Republic)* vol II p 178
[20] Kromholz H, Ruhl F, Schneider W, Schonbach K and Herziger G 1981 *Phys. Lett.* A **82** 82–4
[21] Kies W 1986 *Plasma Phys. Control. Fusion* **28** 1645–57
[22] Krauz V I, Mitrofanov K N, Myalton V V, Khautiev E Yu, Mokeev A N, Vinogradov V P, Vinogradova Yu V, Grabovsky E V and Zukakishvili G G 2007 *Proc. 34th EPS Conf. on Plasma Physics (Warsaw, Poland, 2–6 July 2007)* vol 31F (ECA) P-1.018
[23] Krauz V I, Mitrofanov K N, Myalton V V, Grabovsky E V, Koidan V S, Vinogradov V P, Vinogradova Yu V and Zukakishvili G G 2010 *IEEE Trans. Plasma Sci.* **38** 92–9
[24] Krauz V I, Mitrofanov K N, Myalton V V, Vinogradov V P, Vinogradova Yu V, Grabovsky E V, Zukakishvili G G, Koidan V S and Mokeev A N 2010 *Plasma Phys. Rep. (Russ. J. Fiz. Plasmy)* **36** 937–52
[25] Anan'in S I, Vikhrev V V and Filippov N V 1978 *Fiz. Plazmy (Sov. J. Plasma Phys.)* **4** 315
[26] Vikhrev V V and Braginskii S I 1980 *Reviews of Plasma Physics* vol 10, ed M A Leontovich (Moscow: Atomizdat, 1986 New York: Consultants Bureau) pp 243–315
[27] Gribkov V A *et al* 1989 *Kratk. Soobshch. Fiz. (Sov. J.)* **8** 24 (in Russian)
[28] Bernard A, Coudeville A, Garconnet J P, Jolas A, de Mascureau J and Nazet C 1977 *Proc. 6th Int. Conf. on Plasma Physics and Controlled Nuclear Fusion Research (Berchtesgaden, Germany, 1976)* 47 (Vienna: IAEA) p 113
[29] Scholz M, Miklaszewski R, Gribkov V A and Mezzetti F 2000 *Nukleonika* **45** 155–8
[30] Bruzzone H and Grondonaz D 1997 *Plasma Phys. Control. Fusion.* **39** 1315–26
[31] Bhuyan H, Mohanty S R, Neog N K, Bujarbarua S and Rout R K 2003 *Meas. Sci. Technol.* **14** 1769–76
[32] Andreeshchev E A, Vojtenko D A, Krauz V I, Markoliya A I, Matveev Yu V, Reshetnyak N G and Khautiev E Yu 2007 *Plasma Phys. Rep. (Russ. J. Fiz. Plasmy)* **33** 218–26
[33] Mohammadi M A, Sobhanian S, Ghomeishi M, Ghareshabani E, Moslehi-fard M, Lee S and Rawat R S 2009 *J. Fusion Energy* **28** 371–6
[34] Volobuev I V, Gurei A E, Nikulin V Ya and Polukhin S N 2010 *Plasma Phys. Rep. (Russ. J. Fiz. Plazmy)* **36** 1013
[35] Knoblauch P, Raspa V, Lorenzo F Di, Lazarte A, Clausse A and Moreno C 2010 *Rev. Sci. Instrum.* **81** 093504
[36] Frolov I, Grabovski E, Mitrofanov K, Oleinik G M, Smirnov V P and Zukakishvili G G 2001 *Proc. European Conf. Advanced Diagnostics for Magnetic and Inertial Fusion (Villa Monastero, Varenna, Italy, 3–7 September 2001)* ed P E Stott *et al* (New York: Academic/Plenum) pp 419–22
[37] Glazyrin I V, Grabovski E V, Zukakishvili G G, Karpeev A V, Mitrofanov K N, Oleinik G M and Samokhin A A 2009 *Problems of Atomic Science and Engineering, Ser.'Thermonuclear Fusion' (Russ. J.)* **2** 67–82
[38] Glazyrin I V, Diyankov O V, Karlykhanov N G and Likov V A 2000 *Laser Part. Beams* **18** 261–7
[39] Zukakishvili G G *et al* 2005 *Plasma Phys. Rep. (Russ. J. Fiz. Plasmy)* **31** 908–18
[40] Zukakishvili G G, Mitrofanov K N, Grabovski E V and Olejnik G M 2005 *Plasma Phys. Rep. (Russ. J. Fiz. Plazmy)* **31** 652–64
[41] Filippov N V *et al* 2000 *Czech. J. Phys.* **50/S3** 127–35
[42] Filippov N V *et al* 2000 *Nucleonika* **46** 35–9
[43] Krauz V I, Mitrofanov K N, Myalton V V, Vinogradov V P, Vinogradova Yu V, Grabovsky E V and Koidan V S 2011 *Plasma Phys. Rep. (Russ. J. Fiz. Plasmy)* **38** 742–54
[44] Zielinska E, Paduch M and Scholz M 2011 *Contrib. Plasma Phys.* **51** 279
[45] Babenko A N *et al* 1973 *Plasma Diagnostics* (Moscow: Atomisdat) p 509
[46] Grabovsky E V, Zukakishvili G G, Mitrofanov K N, Oleinik G M, Samokhin A A and Smirnov V P 2002 Fast-acting probes for measurement of magnetic fields in compressed wire arrays Preprint N.0091A *SRC RF TRINITI, Troitsk, Russian Federation*
[47] Kubes P *et al* 2006 *IEEE Trans. Plasma Sci.* **34** 2349–55